Oral presentation | Industrial applications
Industrial applications-III
Tue. Jul 16, 2024 2:00 PM - 4:00 PM Room B

[5-B-02] Total Uncertainty Quantification of the AIAA UQ Challenge Problem using an Interactive Web Browser Based Tool for Data and Automated Workflow Management

*Earl P Duque[1], Michael D Burklund[1], Dave A Amels[1], Steve M Legensky[1] （1. Intelligent Light）

Keywords: Uncertainty Quantification, Aerodynamics, Certification by Analysis

Twelfth International Conference on Computational Fluid Dynamics (ICCFD12), Kobe, Japan, July 14-19, 2024

ICCFD12-2024-5B02

Total Uncertainty Quantification of the AIAA UQ Challenge Problem using an Interactive Web Browser Based Tool for Data and Automated Workflow Management

E.P.N. Duque*, M.D. Burklund*, D.A. Amels*, and S.M. Legensky*
Corresponding author: epd@ilight.com *, Intelligent Light, USA.

1 Introduction

The uncertainty in Computational Fluid Dynamics (CFD) based simulation results may be quantified through rigorous verification, validation and uncertainty quantification (VVUQ) procedures. Procedures and frameworks such as the ASME V&V 20 [1], and Roy-Oberkampf Uncertainty framework [2] require extensive simulations, post-processing workflows and management of the simulation results and experiment data to quantify the contributions of model input uncertainty, numerical uncertainty, and model form uncertainty to the total uncertainty for any given study or design. Engineers need better software tools and computational environments that ease the burden of simulation and data management.

Calls for Certification by Analysis (CbA) of flight systems have become more prevalent in the industry. However, the fluids dynamic community is still wrestling with how to quantity uncertainty for the highly non-linear flow fields associated with flight. In a recent AIAA special session, an Uncertainty Quantification (UQ) Challenge Problem posed to the community as summarized by Cary. et. al. [3]. Participants were asked to use the XFOIL solver [4] to determine whether an airfoil under uncertain model inputs would satisfy specified lift and pitching moment requirements.

Intelligent Light has been developing SpectreUQ - a new computational environment (CE) designed to enable CFD practitioners to easily quantify the total uncertainty in their computational campaigns. It uses a non-intrusive framework that enables the use of any solver. Recently, XFOIL has been included as one of the supported solvers. This extended abstract paper shows the promise of this new CE and reviews the methods used by SpectreUQ to quantity Total Uncertain which consists of Model Input Uncertainty, Numerical Uncertainty, and Model Form Uncertainty. The AIAA UQ Challenge Problem is used as a case study. [3]

2 Problem Statement

2.1 SpectreUQ

Determining the total uncertainty requires rigorous adherence to procedures and frameworks that can require onerous tasks to manage all the data and simulations. SpectreUQ was designed to make it easier to manage the UQ methods and frameworks as outlined in ASME V&V 20 [1], and the Roy-Oberkampf Uncertainty framework [2]. It automates the execution of large scale simulations, post-processing workflows and management of the physical tests and simulation results. Support for XFOIL was coupled into SpectreUQ where model input propagation, discretization error, and model form uncertainty can be evaluated.

2.2 AIAA UQ Challenge Problem

The AIAA UQ Challenge Problem was first introduced by Cary et.al in 2022 [5]. At SciTech 2024, the challenge problem results were presented with several participants from participants and summarized[3]. The problem is motivated by a sailplane airfoil design problem to deliver a payload at a cruise altitude that is sensitive to flight attitude and payload placement on the aircraft. The resulting question is: *Can the payload be delivered under uncertainties associated with flight conditions and the given airfoil.*

The problem specifies a NACA 2412 airfoil with a flap at 70% chord. For cruise attitude, the requirement states that the 0^o angle-of-attack lift coefficient (C_L) be between 0.155 and 0.265 and the0^o angle-of-attack moment coefficient (C_M) be between -0.050 and -0.044.

Parameter	Normal Distribution Characterization	Epistemic Interval Characterization
Angle of Attack	$\mathcal{N}(0.0°,\ 0.1°)$	$\in [-0.3°,\ 0.3°]$
Reynolds Number	$\mathcal{N}(500000,\ 2500)$	$\in [492500,\ 507500]$
Upper Trip location	$\mathcal{N}(0.3c,\ 0.015c)$	$\in [0.255c,\ 0.345c]$
Lower Trip location	$\mathcal{N}(0.7c,\ 0.021c)$	$\in [0.637c,\ 0.763c]$
Flap deflection	$\mathcal{N}(0°,\ 0.08°)$	$\in [-0.24°,\ 0.24°]$

Table 1: UQ Challenge Problem input uncertainties.

The problem was assumed to be low speed such that Mach number did not have a influence on the problem. Five model input parameters were identified as important: angle-of-attack, Reynolds number, upper trip location, lower trip location and flap deflection angle. Probabilistic normal distribution characterizations and epistemic interval characterizations were provided as shown in Table 1. Participants were asked to evaluate using purely probabilistic model inputs (aleatory), purely epistemic or mixed (aleatory and epistemic) inputs. Finally, grid refinement studies were also requested whereby the participants could perform "grid refinement" studies by changing the number of panels used to discretize the airfoil surface in XFOIL.

3 Total UQ Methodologies with XFOIL

In this section, the methods to determine model input uncertainty, numerical uncertainty, and model form uncertainty are presented and demonstrated using the XFOIL code. Furthermore, the simulations and post-processing are performed outside of SpectreUQ first to illustrate the complexity in performing the UQ workflows.

3.1 XFOIL

Simulations were performed using a special version of XFOIL [**?**] that was created by the Challenge Problem committee. This version supports increased floating point precision in the output and increases the number of panels allowed in the airfoil definition. A NACA2412 profile was specified using the internal default XFOIL profile. Simulations were performed on a Windows 10 host using an Intel(R) Xeon(R) CPU E5-2687W 0 @ 3.10GHz with 64GB of RAM. Simulations that support both panel refinement and model input propagation were performed. "Experiment" data statistics were derived from the results of the challenge problem participants to illustrate the model form uncertainty method.

3.2 Model Input Propagation

Model Input Propagation methodologies systematically sample combinations of the inputs to the solver in order to determine the effective resulting uncertainty. The sampling is determined by first characterizing model inputs as either aleatory or epistemic. Aleatory model input parameters are those parameters characterised by a known probabilistic distribution. Epistemic inputs do not have a known distribution and are often expressed as an interval that is sampled. Monte Carlo and Latin Hypercube sampling methods are often used. These have the downside of requiring a large number of samples resulting in a large number of expensive simulations. Surrogate modeling approaches such as Polynomial Chaos Expansion have been used as alternate methods that reduce the number of samples. In these methods, a smaller number of samples are performed and used to build a model that can then be more extensively sampled to determine the statistics of the quantities of interest (QoI) i.e. Lift, Drag, Pitching Moments. The QoI are then viewed using Probability Density Function or Cumulative Distribution Function (CDF) Plots.

Figure 1 shows an example CDF of the Lift Coefficient for the NACA2412 Airfoil using a Non-Intrusive Polynomial Chaos Expansion (NIPCE) sampling [6] and XFOIL with 364 panels. The x-axis represents values of the QoI, C_L, and the y-axis represents the cumulative probability. For example the value $C_L = 0.25$ has the probability of occurring approximately 92% of the time.

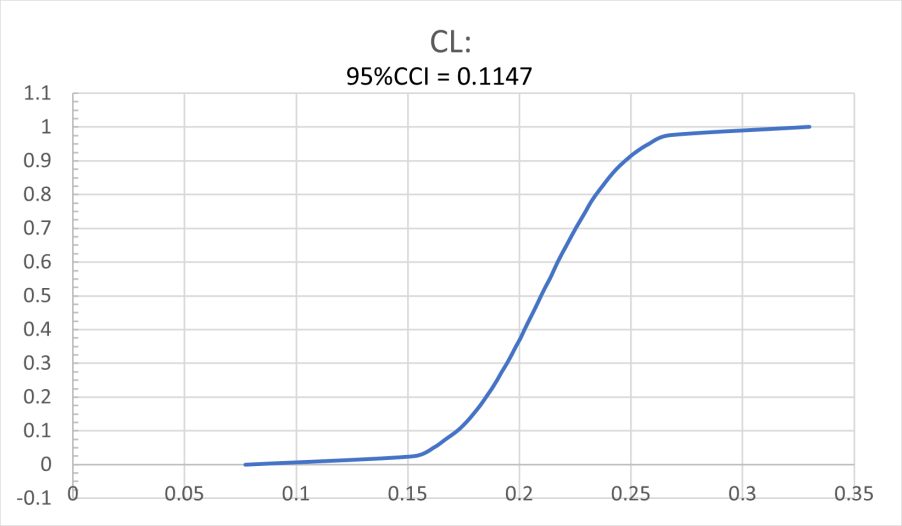

Figure 1: Example Cumulative Distribution Function of C_L for the NACA2412 Airfoil Pure Aleatory Propagation using NIPCE, Sampling using XFOIL with 364 panels mean parameter inputs of alpha=0-degrees, Re=500,000, Upper-Transition=0.3%c, Lower-Transition=0.7%c)

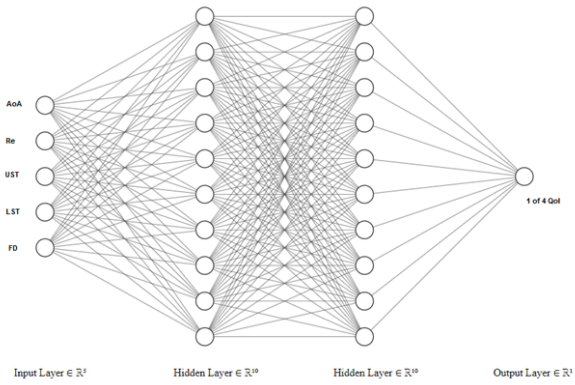

Figure 2: One of four CNN designs for angle-of-attack, Reynolds Number, Upper/Lower Transition Locations and Flap Deflection Angle for the aleatory propagation. Each of the four network outputs produce a since Quantities of Interest (C_L, C_D, C_{Dp} and C_M)

3.2.1 Convolutional Neural Network surrogate.

A non-PCE approach for creation of the surrogate model is to use a convolutional neural network (CNN) which is trained on the solver input parameters and resulting QoIs. Figure 2 presents a schematic of a network investigated using the input parameters of Angle of Attack, Reynolds Number, Upper Airfoil Trip Point, Lower Airfoil Trip Point, and Flap Defection angle as inputs for training while the resulting QoIs (Lift, Drag, Pitching Moments) were used for the truth data for training. Four separate networks can be trained independently, one for each of the QoIs.

One measure of model accuracy is to check the resulting MSE (mean squared error) of the predicted QoI to the training QoI truth data. For the magnitude of the data for the QoIs in this investigation $MSE < 1e^{-9}$ is considered successful training of the surrogate. This method is used in place of the traditional NIPCE surrogate model in the results shown below.

3.2.2 Sensitivity

Sensitivity analysis is an additional outcome resulting from the model input propagation methods and can show the relative effect of a model input into the various quantities of interest. Sobel indexes is one method used to illustrate sensitivity.[7]

Figure 3 shows one example presenting the Sobel index illustrating the sensitivity of integrated QoI

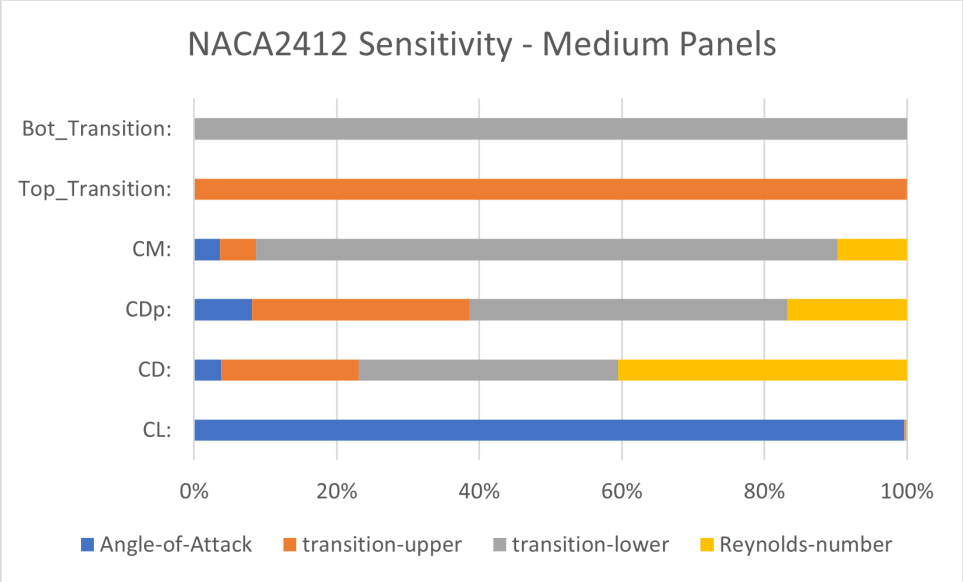

Figure 3: Sobel indices showing sensitivity of system response quantities C_L, C_D ,C_{D_p}, Transition to Turbulence to the model input parameters - angle-of-attack, Reynolds number, and upper/lower airfoil transition point specification for the NACA2412 Airfoil as predicted with XFOIL using 182 panels

(pitching moment, drag and lift coefficients) to model inputs Angle of Attack, Reynolds Number and transition point location. This figure shows that the Lift Coefficient is mainly sensitive to the angle of attack. Drag Coefficient is affected mainly by the Reynolds Number and then the transition point location with the lower transition point having a greater influence. The Pressure Drag Coefficient is less influenced by the Reynolds Number. Perhaps surprising is that the pitching moment is most sensitive to the transition point on the lower surface.

3.3 Numerical Uncertainty via Grid (Panel) Refinement

The Numerical Uncertainty of the C_L, C_D, C_{D_p} and C_M were determined using the methods as outlined in the ASME VV20 [1], Celik et.al. [8], Eca [9] and by Roache [10] and outlined below.

The representative grid size, h_i, is first determined by equation 1 where i=1-fine, 2-medium, 3-coarse panel distributions and N is the number of panels used in the XFOIL simulation.

$$h_i = \frac{1}{N} \tag{1}$$

where i=1 is the finest and i=3 is the coarsest number of panels.

The relative refinement level is then determined by equation 2

$$r_{ij} = \frac{h_i}{h_j} \tag{2}$$

Once the relative refinement is known, then the observed order of accuracy, p, is calculated by equation 3.

$$p = \frac{1}{ln(r_{21})} \left| ln \left| \frac{\varepsilon_{32}}{\varepsilon_{21}} \right| + q(p) \right| \tag{3}$$

where the function $q(p)$ is iteratively computed via equation 4.

$$q(p) = ln(\frac{r_{21}^p - s}{r_{32}^p - s}); s = sig(\varepsilon_{32}/\varepsilon_{21}) \tag{4}$$

The extrapolated exact value can be determined using either the relative fine and medium panel distribution as shown in equation 5 or the medium and coarse panel distribution, equation 6 as presented by Celik [8]).

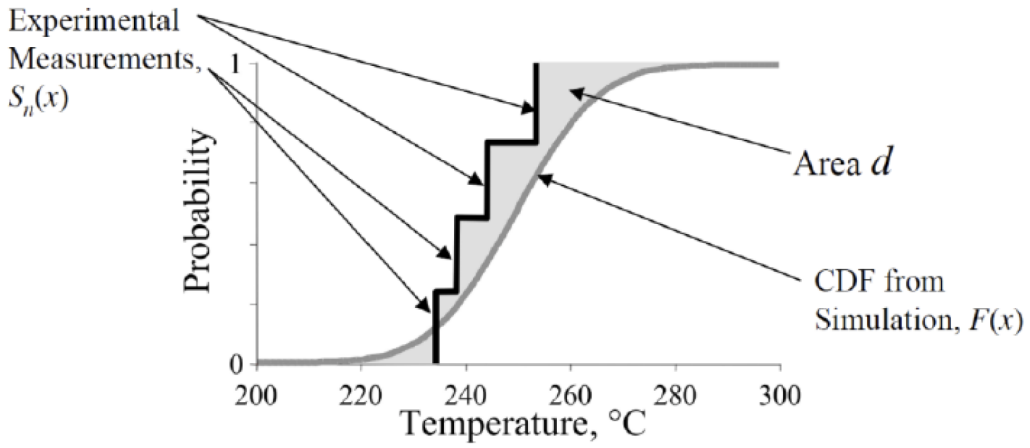

Figure 4: Example Overlay of *Truth Data* with simulation CDF (reproduced from [14])

$$\phi_{ext}^{21} = \left(\frac{r_{21}^p \phi_1 - \phi_2}{r_{21}^p \phi_1 - 1}\right) \tag{5}$$

$$\phi_{ext}^{32} = \left(\frac{r_{32}^p \phi_2 - \phi_3}{r_{32}^p \phi_2 - 1}\right) \tag{6}$$

More than three panel refinements could be used in a study and combinations of the relative refinement levels can be used. The discretization errors should be determined based upon the panel refinement level upon which the model input propagation was performed. For example, if a set of four panel refinements were performed (i.e. coarse, medium, fine and extra-fine) panels and the model inputs were propagated on the medium grid, then the numerical uncertainty could be determined by using the medium, fine and extra-fine panels as the k=3,2,1, respectively.

The numerical error comprises of the discretization and iterative error. Once the Observed Order, p, is known for $p>1$, equation 7 is used to determine the discretization error. Otherwise, equation 8 is used.

$$U_{Diss} = \left|\frac{1.25(\phi_1 - \phi_2)}{r_{21}^p - 1}\right|; p > 1 \tag{7}$$

$$U_{Diss} = |3(\phi_3 - \phi_1)| \tag{8}$$

3.4 Model Form Uncertainty (MFU)

Simulation validation studies evaluate how accurately a simulation models the real world by comparing the simulated results to trusted *truth data*. This data can be either experiment or high fidelity simulation data. Whiting et.al. evaluated four different methods - Area Validation Metric (AVM) [11], Modified Area Validation Metric (MAVM) [12], ASME V&V20 [1], and a Bayesian method by Kennedy and O'Hagen [13].

The present method uses the AVM method which provides a method to estimate the displacement to either side of the CDF by taking difference of the the simulation data ($F(x)$) and the *Truth Data* ($S_n(x)$) . In this case the **truth data** is presented in the CDF plots along with the simulation data. Figure 4 shows the overlay of typical experiment data over the simulation CDF.

The area d is then computed as:

$$d = \int_{-\infty}^{+\infty} |F(Y) - S_n(Y)|\, dY \tag{9}$$

where $F(Y)$ is the truth data and $S_n(Y)$ is the aleatory propagation of simulation inputs or for mixed uncertainty is the aleatory propagation of the mean epistemic inputs.

The area,d, is then added to the left and the right of the CDF creating an interval of uncertainty as shown in Figure 5.

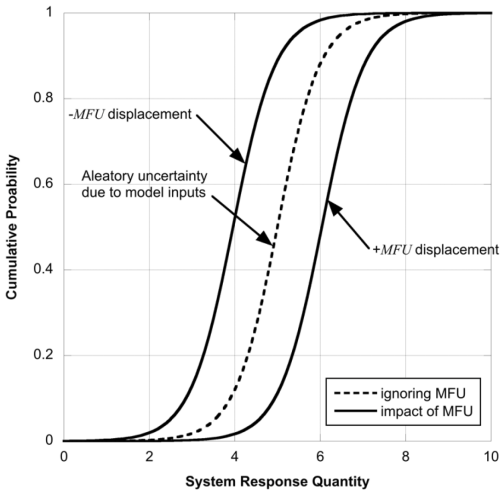

Figure 5: The impact of MFU upon the CDF, Creates an interval of uncertainty to the probabilistic response (reproduced from [14])

3.5 Total Uncertainty

The *Total Uncertainty* accounts for all three types of uncertainty as presented above, Module Input Uncertainty as determined via model input propagation methods, Numerical Uncertainty as determined via grid convergence methods and Model Form Uncertainty via Area Validation Metric. These uncertainties are cumulatively added to arrive at the Total Uncertainty which provides an interval of uncertainty that can be displayed via a *P-Box* plot. This method follows the Uncertainty Quantification Framework as presented by Roy and Oberkampf [2]. Of note is the "Conservative Confidence Interval" (CCI) which is defined as the interval between 2.5% and 97.5% probability. Then by overlaying objective parameters such as target Lift and Moment ranges, one can determine the likelihood that a device might exceed those targets.

4 Results

The following presents each of the uncertainties - Model Input, Numerical, Model Form - leading up to the TotalUQ.

4.1 Model Input Propagation

Model Inputs were propagated with XFOIL using the input parameters as presented in Table 1. Two propagation schemes were evaluated - pure aleatory and mixed (Aleatory and Epistemic). The CNN surrogate model methods was used to propagate the aleatory parameters. For the mixed uncertainty, the aleatory parameters were angle-of-attack, Reynolds Number, upper and lower turbulence transition location while the flap deflection angle was treated as a uniformly sampled epistemic interval.

4.1.1 Pure Aleatory

Figure 6 presents the CDF of C_L and C_M for the pure aleatory model input propagation. The blue line is the CDF while the green line represents to minimum and maximum design limits as stated by the UQ Challenge Problem. The C_L shows that there is there is high probability that the C_L requirement will be met since the CDF is contained within the desired interval. For the C_M, the left and right tails of the distribution are starting to exceed the limits. Therefore, this shows that for pure aleatory model inputs C_L and C_M may be satisfied.

4.1.2 Mixed Uncertainty

Figure 7 shows the results when the flap deflection is considered as epistemic interval. In this case, each flap deflection angle is held constant while the other four model input parameters are propagated as

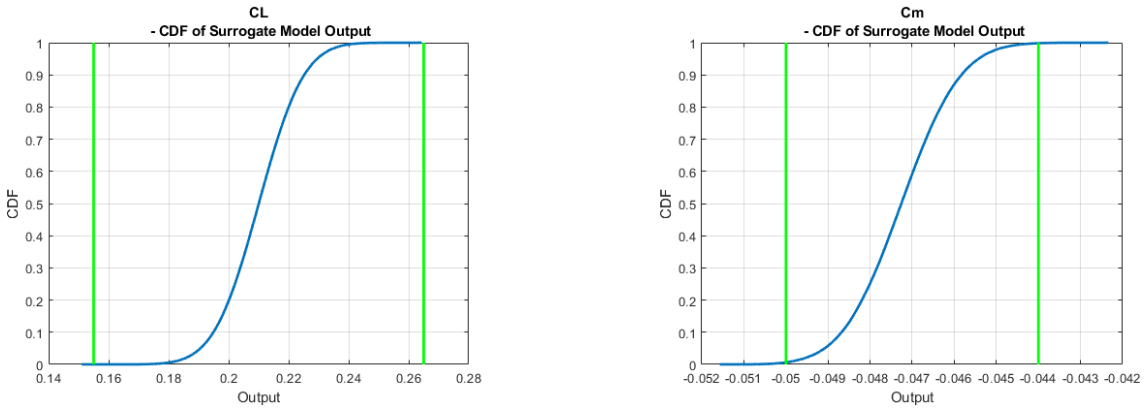

(a) C_L (b) C_M

Figure 6: Pure Aleatory CDF of Lift and Moment Coefficient (Blue Line) and Design Constraints (Green)

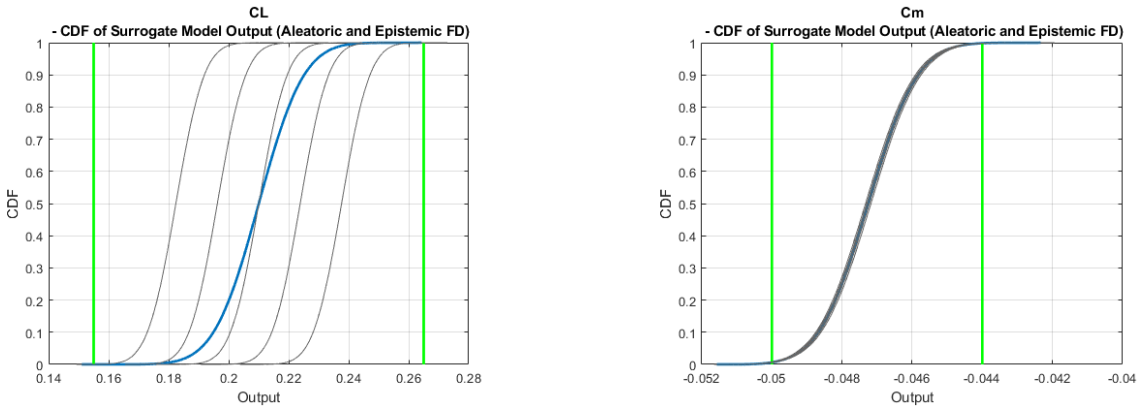

(a) C_L (b) C_M

Figure 7: Mixed Uncertainty CDF for Lift and Moment Coefficient, Aleatory(AoA, Turbulence Transition, Reynolds Number), Epistemic(Flap Deflection) , Green Line Delineates the Design Constraints

aleatory. Each epistemic evaluation is shown as a grey line and the pure aleatory propagation is shown in blue for reference. The C_L CDF plot shows that each flap deflection angle causes the CDF plot to shift accordingly. The main effect is that these shifts causes an interval probability of an answer. For example, at a 90% probability the C_L will be within the range of approximately 0.19 and 0.245. For C_M, the CDF's show that there is less effect upon the probability distribution resulting in a small interval within the flap deflection interval.

4.1.3 Sensitivity

Figure 8 presents the Sobel Index sensitivity plot showing the effect of the 5 parameter aleatory inputs of Flap Deflection angle (FD), Reynolds Number (Re), Upper and Lower Transition point (UST and LST, respectively) and angle-of-attack (AoA) upon the airfoil pitching moment Lift (C_L), Pressure Drag (C_{Dp}), Total Drag Coefficient (C_D), and Pitching Moment (C_m). It shows that the C_M is dominated by the flap deflection. The C_L is mostly affected by the flap deflection and angle-of-attack. The drag is somewhat affected by the the flap deflection. However the upper and lower turbulence transition dominate both the pressure drag and the total drag coefficient.

4.2 Grid Refinement

A total of four panel refinements were performed with successive panel doubling from very coarse (128 panels) to extra fine (1024 panels). Flow conditions were set at the mean conditions of 0^o angle-of-attack, Reynolds number of 500,000, upper transition set to 30% of chord and lower transition set to 70% of chord and with 0^o flap deflection. Tables 2 and 3 present the observed order of accuracy (OOA), grid

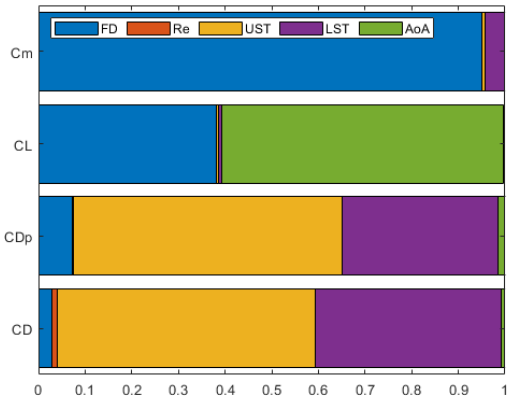

Figure 8: Sobel Index Plot showing sensitivity of Cm, CL, CDp, CD to Flap Deflection (FD), Reynolds Number (Re), Upper/Lower Transition (UST,LST) and Angle of Attack (AoA)

	OOA	GCI_{32}	S_{ext}	U_{Diss}	$\varepsilon_{32/\varepsilon_{21}}$
C_L	-1.2635	0.0014358	0.22698	0.00045764	-2.4007
C_D	-3.5013	0.00031808	0.008939	6.2393e-06	11.3235
C_{D_P}	-2.8901	0.035431	0.00074614	6.9509e-05	7.4176
C_M	-1.3744	0.0014501	-0.049726	0.00010465	-2.5186

Table 2: NACA2412 Observed Order of Accuracy (OOA), Grid Convergence Index (GCI), Observed Error (Error), with Coarse, Medium and Fine Panel distributions using XFOIL (alpha=0-degrees, Re=500,000, Upper-Transition=0.3c, Lower-Transition=0.7c

convergence index between the coarse-medium (GCI_{32}) and fine-extra fine grids (GCI_{21}), respectively, the extrapolated scalar result S_{ext}, the discretization error U_{Diss} and the ratio of the relative differences.

These results show that the the Coarse, Medium, Fine resolutions exhibit oscillatory convergence as indicated by the negative OOA. Figure 9 illustrates this behaviour. On the contrary, the Medium, Fine, extra Fine resolution exhibits that the results has converged as evidenced by the OOA and GCI values. Figure 10 shows how the fine to extrafine has plateaued to the exact solution. Figure 11 adds the grid error to the Mixed Uncertainty CDF for C_L and C_M illustrates the effect of grid error and shows that it has a small effect upon the uncertainty interval.

4.3 Model Form Uncertainty

Figure 12 adds in the model form uncertainty (MFU) to the CDF. The orange line illustrates data that was extracted from the UQ Challenge results and used as synthesized experiment data. The MFU quantity, d, was then computed and added as an increment to the independent axis of the CDF plots and shown in cyan. In addition, Figure 13 presents a semilog-y plot of the CDF which helps to highlight

	OOA	GCI_{21}	S_{ext}	U_{Diss}	$\varepsilon_{32/\varepsilon_{21}}$
C_L	NaN	0	0.20991	0.00045764	∞
C_D	NaN	0	0.0089166	6.2393e-06	∞
C_DP	NaN	0	0.00095044	6.9509e-05	∞
C_M	NaN	0	-0.047234	0.00010465	∞

Table 3: NACA2412 Observed Order of Accuracy (OOA), Grid Convergence Index (GCI), Observed Error (Error), with Medium, Fine and Extra Fine Panel distributions using XFOIL (alpha=0-degrees, Re=500,000, Upper-Transition=0.3c, Lower-Transition=0.7c

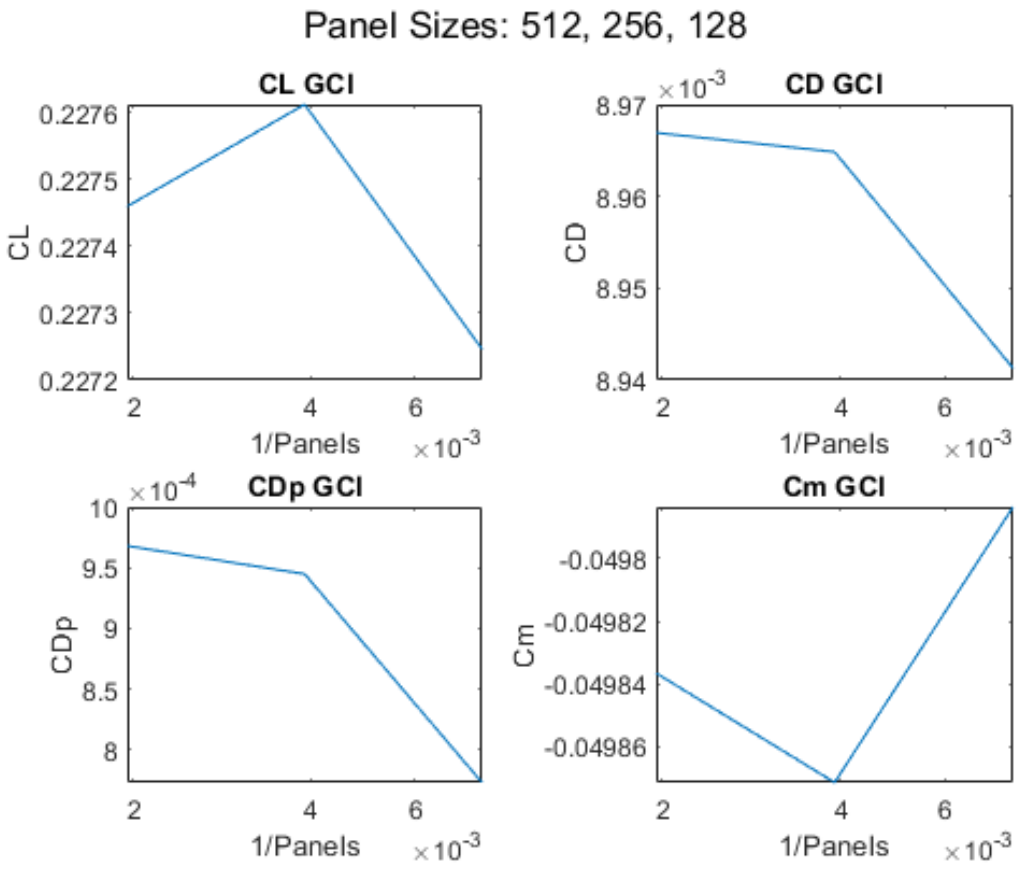

Figure 9: Grid Convergence Coarse, Medium,Fine Grid Refinement

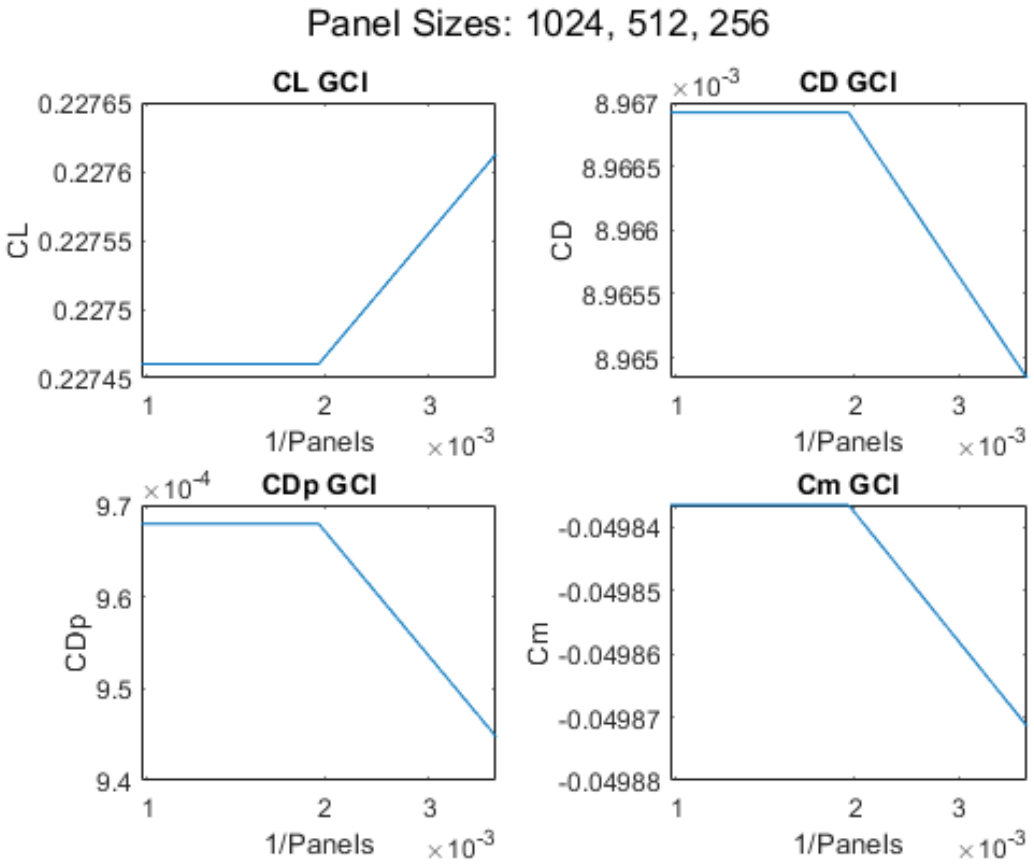

Figure 10: Grid Convergence Medium,Fine, Extra Fine Grid Refinement

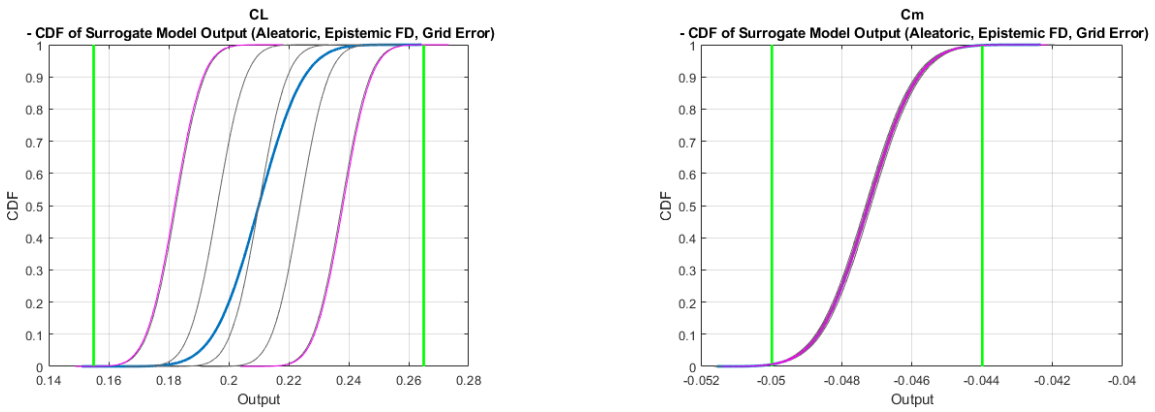

(a) C_L (b) C_M

Figure 11: Mixed Uncertainty CDF for C_L and C_M, Aleatory(AoA, Turbulence Transition, Reynolds Number), Epistemic(Flap Deflection) , Green Line Delineates the Design Constraints, Mean Distribution (Blue Line), Grid Convergence Error (Magenta Line), Experiment Data Distribution(Orange Line), Design Constraint (Green Line)

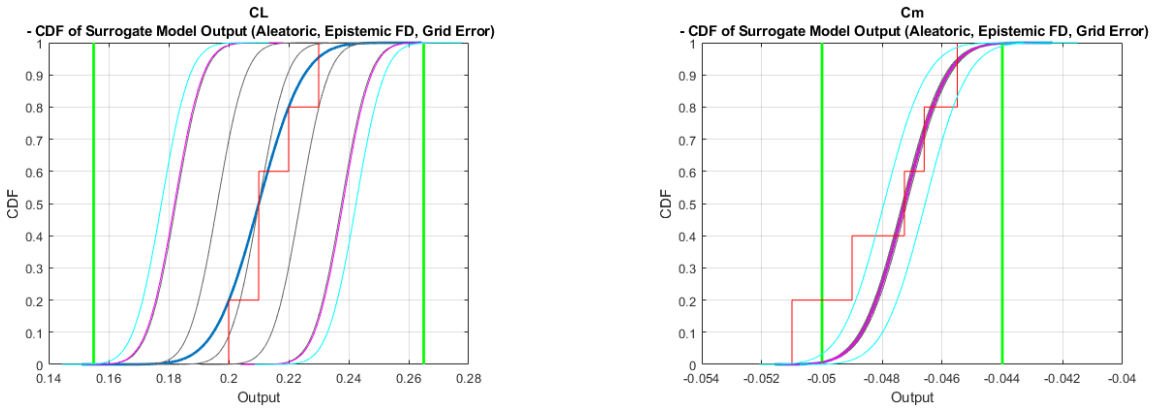

(a) CL (b) CM

Figure 12: Mixed Uncertainty CDF for Lift and Moment Coefficient with MFU, Aleatory(AoA, Turbulence Transition, Reynolds Number), Epistemic(Flap Deflection) , Green Line Delineates the Design Constraints, Mean Distribution (Blue Line), Grid Convergence Error (Magenta Line), MFU (Cyan Line), Experiment Data Distribution(Orange Line), Design Constraint (Green Line)

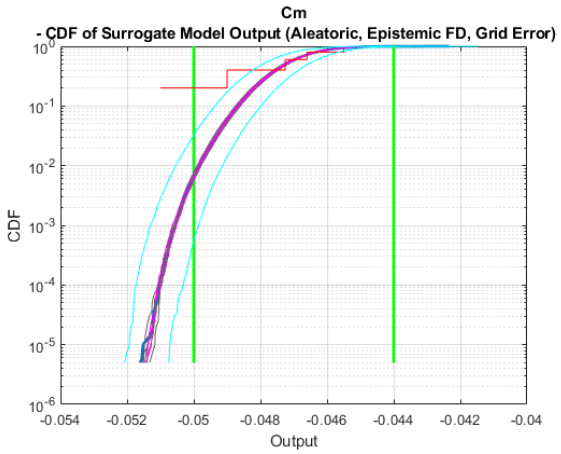

Figure 13: SemiLog-y CDF plot of C_M highlights the left tail

the left side tail of the distribution plot. It shows that there is a definite possibility to exceed the lower limit of the design contraint. The Total UQ plot will present the extent of that possibility.

4.4 Total UQ

The Total Uncertainty (TotalUQ) adds all the uncertainties (model input, discretization error, and model form). Figure 14 shows the CDF and highlights the 95% conservative confidence interval (CCI) which is the interval between 2.5% and 97.5% probability of the total uncertainties. The CCI shows that the C_L remains within the bounds of the design constraints. The C_M on the other hand shows that there is low (2.5%) probability that the C_M may exceed the lower design constraint. The main contribution to the uncertainty is the MFU since there is not much effect from the epistemic interval contribution from the Flap Deflection or from the discretization error. This result indicates that more experiment data may be useful to gain a better understanding of the model form error and could be used to help reduce the model form error. In addition, other contributions inherent to the solver besides the discretization error can contribute to the model form, such as the choice of turbulence model parameters. The choice of modeling methodologies could change the shape of the probabilistic curves. By obtaining better/more experiment data and by performing more simulations, one could gain more confidence how well the airfoil would satisfy the design constraints.

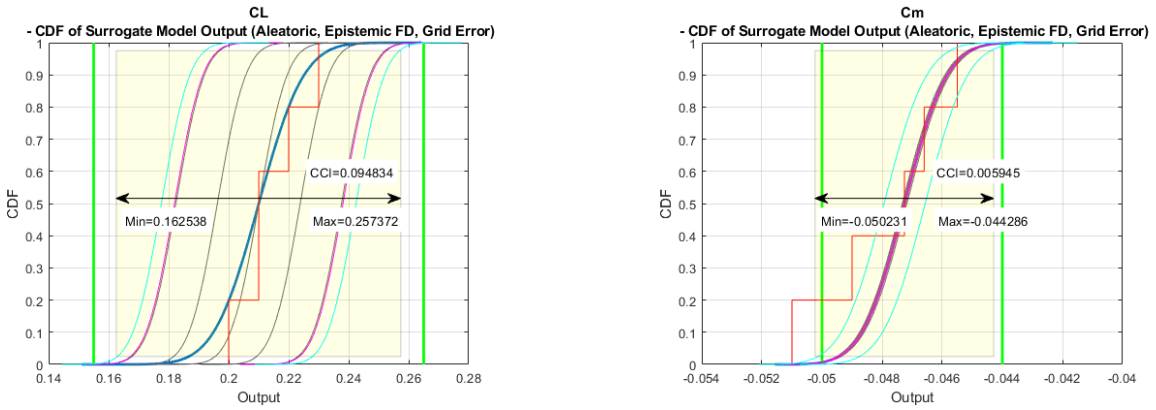

(a) C_L (b) C_M

Figure 14: Mixed Uncertainty CDF for Lift and Moment Coefficient, Aleatory(AoA, Turbulence Transition, Reynolds Number), Epistemic(Flap Deflection) , Green Line Delineates the Design Constraints

4.5 SpectreUQ

SpectreUQ with the XFOIL solver was used to perform the mixed uncertainty specification as outlined above. For the conference presentation, video of a working version of SpectreUQ will be shown that uses the TotalUQ framework presented but implemented in a UI that guides engineers through the problem setup and exploration of the results. Figure 15 presents a result from SpectreUQ that highlights the ability to explore the Probability Density Function (PDF) and CDF of the pressure coefficient and skin friction on the airfoil surface.

5 Summary and Future Work

Uncertainty Quantification methods can be used to help determine the likely hood that a design will meet design constraints through the systematic use of simulations and truth data (i.e. wind tunnel data). The AIAA UQ Challenge Problem presented a case study that utilized the XFOIL solver to determine if an airfoil (NACA2412) with a flap deflection would meet the lift and pitching moment design constraints under uncertain flight conditions. The UQ methods that are used by Intelligent Light's new computational environment, SpectreUQ, was presented in this extended abstract. The methods showed that when including a mixed uncertainty propagation whereby the angle-of-attack, turbulence transition location, and Reynolds Number are treated a aleatory inputs and the flap deflection angle treated as epistemic, that the pitching moment had a 2.5% probability of exceeding the lower C_M design limit mainly due to the model form uncertainty. This then lead to the recommendation for better/more experiment data and/or exploring different modeling methods (i.e. turbulence model) to reduce the model form uncertainty. A demo of the software was presented at the ICCFD conference which demonstrated how this new CE can be used to make it easier for engineers to setup, execute, and explore their UQ studies.

6 Acknowledgements

This material is based upon work supported by the U.S. Department of Energy, Office of Science, Office of Advancing Computing Research under Award Number DE-SC0015162.

Figure 15: Example Exploration of SpectreUQ Determined PDF and CDF

References

[1] Hugh Coleman and Committee Members. *ASME VV 20-2009 Standard for Verification and Validation in Computational Fluid Dynamics and Heat Transfer (VV20 Committee Chair and principal author)*. 01 2009.

[2] Christopher J Roy and William L Oberkampf. A comprehensive framework for verification, validation, and uncertainty quantification in scientific computing. *Computer methods in applied mechanics and engineering*, 200(25-28):2131–2144, 2011.

[3] Andrew W Cary, John A Schaefer, Erin C DeCarlo, Earl P Duque, and Manas Khurana. Overview of fluid dynamics uncertainty quantification challenge problem and results. In *AIAA SCITECH 2024 Forum*, page 0705, 2024.

[4] Mark Drela. Xfoil: An analysis and design system for low reynolds number airfoils. In *Low Reynolds number aerodynamics*, pages 1–12. Springer, 1989.

[5] Andrew W Cary, John Schaefer, Earl P Duque, Manas Khurana, and Erin C DeCarlo. Overview of challenges in performing uncertainty quantification for fluids engineering problems. In *AIAA SCITECH 2022 Forum*, page 2357, 2022.

[6] Michael Eldred. Recent advances in non-intrusive polynomial chaos and stochastic collocation methods for uncertainty analysis and design. In *50th AIAA/ASME/ASCE/AHS/ASC Structures, Structural Dynamics, and Materials Conference 17th AIAA/ASME/AHS Adaptive Structures Conference 11th AIAA No*, page 2274, 2009.

[7] IM Soboĺ. Sensitivity estimates for nonlinear mathematical models. *Math. Model. Comput. Exp.*, 1:407, 1993.

[8] Ishmail B Celik, Urmila Ghia, Patrick J Roache, and Christopher J Freitas. Procedure for estimation and reporting of uncertainty due to discretization in cfd applications. *Journal of fluids Engineering-Transactions of the ASME*, 130(7), 2008.

[9] L Eça and M Hoekstra. Evaluation of numerical error estimation based on grid refinement studies with the method of the manufactured solutions. *Computers & Fluids*, 38(8):1580–1591, 2009.

[10] Patrick J Roache. Verification of codes and calculations. *AIAA journal*, 36(5):696–702, 1998.

[11] Scott Ferson, William L Oberkampf, and Lev Ginzburg. Model validation and predictive capability for the thermal challenge problem. *Computer Methods in Applied Mechanics and Engineering*, 197(29-32):2408–2430, 2008.

[12] Ian T Voyles and Christopher J Roy. Evaluation of model validation techniques in the presence of uncertainty. In *16th AIAA Non-Deterministic Approaches Conference*, page 0120, 2014.

[13] Marc C Kennedy and Anthony O'Hagan. Bayesian calibration of computer models. *Journal of the Royal Statistical Society: Series B (Statistical Methodology)*, 63(3):425–464, 2001.

[14] Nolan W Whiting, Christopher J Roy, Earl Duque, Seth Lawrence, and William L Oberkampf. Assessment of model validation, calibration, and prediction approaches in the presence of uncertainty. *Journal of Verification, Validation and Uncertainty Quantification*, 8(1):011001, 2023.